Influence of Membrane Components in the Binding of Proteins to Membrane Surfaces†

Finly Philip and Suzanne Scarlata*

Department of Physiology & Biophysics, State University of New York at Stony Brook, Stony Brook, New York 11794-8661

Received March 30, 2004; Revised Manuscript Received July 8, 2004

ABSTRACT: We have quantified the enhancement of membrane binding of activated and deactivated $G\alpha_s$ and $G\alpha_q$ subunits, $G\beta\gamma$ subunits, and phospholipase $C\beta_2$ by lipid rafts and by the presence of membrane-associated protein partners. Membrane binding studies show that lipid rafts do not affect the intrinsic membrane affinity of $G\alpha_q$(GDP) and $G\alpha_s$(GDP), supporting the idea that these proteins partition evenly between the domains. Visualization of lipid rafts on monolayers by use of a probe that does not enter raft domains shows that neither activated nor deactivated $G\alpha_q$(GDP) subunits distribute evenly between the raft and nonraft domains, contrary to previous suggestions. Membrane binding of deactivated $G\alpha_q$ and $G\alpha_s$(GDP) became weaker when $G\beta\gamma$ subunits were present, in contrast with the behavior predicted by thermodynamics. However, activated $G\alpha$ subunits and phospholipase $C\beta_2$ were recruited to membrane surfaces by protein partners by predicted amounts. Our studies suggest that the anomalous behavior seen for deactivated $G\alpha$ subunits in the presence of $G\beta\gamma$ subunits may be due to conformational changes in the N-terminus and/or occlusion of a portion of its membrane interaction region by $G\beta\gamma$. Even though membrane recruitment was clearly observed for one protein partner, the presence of a second partner of lower affinity did not further promote membrane binding. For these proteins, the formation of larger protein complexes with very high membrane affinities is unlikely.

Many proteins bind transiently to membrane surfaces to interact with target proteins. The targeting of a cytosolic protein to a membrane may result from several factors including the exposure of the membrane binding interface due to dissociation of a subunit or cofactors, the binding of Ca^{2+}, the attachment of hydrophobic moiety such as palmitoyl, conformational changes brought about by phosphorylation, or recruitment of the protein by a newly released partner on the membrane surface. For example, light activation of rhodopsin causes the exchange of GDP for GTP on $G\alpha_t$, which changes the conformation of its myristoylated N-terminus, reducing its affinity for membrane-bound $G\beta\gamma$ subunits (see ref *1*, and for review see ref *2*). These changes result in release from the membrane so that it may interact with cytosolic effectors. Other G protein systems may also use transient membrane association/dissociation events. Another example is the reported recruitment of β-adrenergic receptor kinase to the membrane surface by newly released $G\beta\gamma$ subunits after receptor activation. This membrane recruitment localizes the β-adrenergic receptor to its target receptor, promoting desensitization (see ref *3*). The ability of G proteins to change their attachment to the membrane is expected to vary depending on their mechanism of activation and deactivation. Permanent attachment of G proteins to the membrane surface would keep them localized to their receptors ready for activation, while transient membrane attachment may help to downregulate signals when G protein effectors are integral membrane proteins.

Adding to the complexity of membrane recruitment of G proteins and effectors by protein partners is the possibility that membrane binding may also be promoted by secondary interactions with other proteins in their signaling pathway. For example, RGS4, whose function is to accelerate the GTPase activity of $G\alpha$ subunits, binds strongly not only to activated $G\alpha_q$ subunits but also to other proteins that interact with $G\alpha_q$, such as phospholipase $C\beta_1$ ($PLC\beta_1$),[1] as well as $G\beta\gamma$ subunits (*4*). The ability of a signaling protein to have multiple interaction sites may serve some role in the formation of higher-order signal transduction complexes on membrane surfaces.

Besides membrane recruitment of a protein by partners, it is possible that the membrane surface itself may play a role. The membrane binding characteristics of G proteins have been previously reported. In general, both $G\alpha$ and $G\beta\gamma$ subunits have positively charged lobes that allow for interaction with negatively charged lipids (*5*, *6*). Additionally, irregularities on the membrane surface may affect the distribution of membrane-associated proteins, which may promote protein interactions that in turn affect the binding stability. Previous studies have indicated that the presence

† This work was supported by a Grant-in-Aid from the American Heart Association (015051N) and by the National Institutes of Health General Medicine GM 53132.

* Corresponding author: phone 631-444-3071; fax 631-444-3432; e-mail Suzanne.Scarlata@sunysb.edu.

[1] Abbreviations: $PLC\beta$, mammalian phosphoinositide-specific phospholipase C type β; $PI(4,5)P_2$, phosphatidylinositol 4,5-bisphosphate; Laurdan, 6-lauroyl-2-(dimethylamino)naphthalene; Dabcyl SE, 4-(dimethylamino)phenylazophenyl-4-benzoic succinimidyl ester; Coumarin, 7-(dimethylamino)coumarin-4-acetic acid succinimidyl ester; POPC, 1-palmitoyl-2-oleoylphosphatidylcholine; POPS, 1-palmitoyl-2-oleoylphosphatidylserine; SM, egg sphingomyelin; Ch, cholesterol.

10.1021/bi049381+ CCC: $27.50
Published on Web 08/28/2004

of liquid-ordered domains in fluid-phase model membranes (i.e., rafts) affected the distribution of G$\beta\gamma$ subunits (*7*). Model membranes containing lipid rafts can be prepared from lipids with at least one saturated chain by increasing the cholesterol above 33 mol % (*8*). The presence of lipid rafts may affect the binding and distribution of G protein subunits in two ways. First, if membranes containing rafts are prepared from cholesterol mixed with lipids that have anionic headgroups, then the charge density in the fluid phase regions will be higher than if the lipids and cholesterol were uniformly mixed. Second, proteins that are modified with saturated hydrocarbon chains may become kinetically trapped in the well-packed liquid ordered phase, whereas proteins that are modified with unsaturated hydrocarbon chains would tend to be excluded from rafts (see refs *9*−*11*). In either case, the presence of rafts would have the effect of decreasing the area of the membrane into which the protein binds and in turn result in an apparent decrease in the membrane partition coefficient.

In this study, we have examined the ability of one or more membrane-bound proteins to recruit their partners to the membrane surface. Since we are using G proteins as test cases for this study, and these proteins are modified by saturated (Gα subunits) and unsaturated (G$\beta\gamma$ subunits) hydrocarbon chains, we have also determined the role of lipid rafts in localizing these proteins to particular areas of the membrane, thereby increasing their local concentration (see ref *12*). We have previously measured the membrane binding affinities of $G\alpha_q$, $G\beta_1\gamma_2$, and their effector phospholipase Cβ (PLCβ) to model membrane surfaces (*13*, *14*). PLCβ is an effector for both $G\alpha_q$ and G$\beta\gamma$ subunits, and the affinities between PLCβ (for reviews see refs *15* and *16*) and activated and deactivated (i.e., GDP-bound and GTPγS-bound) $G\alpha_q$ and between PLCβ and G$\beta\gamma$ subunits have been reported, as have the affinities $G\alpha_q$(GDP)−G$\beta\gamma$ and $G\alpha_q$(GTPγS)−G$\beta\gamma$ (*14*, *17*). Using these proteins, along with $G\alpha_s$ for comparison, we have quantified the role of protein partners and membrane domains in their recruitment to the membrane surface. We find that while membrane recruitment of Gα(GTPγS), G$\beta\gamma$, and PLCβ occurs in a manner predicted by thermodynamics, the presence of protein partners decreases the affinity of Gα(GDP). The presence of rafts does not appear to affect membrane partitioning of these proteins.

MATERIALS AND METHODS

Lipids. All lipids were purchased from Avanti Polar Lipids, Inc. Lipids were dried to a thin film in a small pear-shaped flask by use of a rotary evaporator. Dried lipids were suspended in 150 mM NaCl and 20 mM Hepes (pH 7.2) buffer to give a concentration of 2 mM and then taken through 10 alternating freeze−thaw cycles with liquid nitrogen and a 37 °C water bath. Large unilamellar vesicles (LUVs) were freshly prepared by extrusion through 100 nm pore filter before every experiment.

Proteins. Expression and purification of recombinant $G\alpha_q$, His_6-$G\beta_1\gamma_2$, and PLCβ_2 through baculovirus infections of SF9 cells have been described previously (*13*, *14*). $G\alpha_s$ was purified from SF9 cells following the methods used for $G\alpha_q$ purification. This expression system allows for postsynthetic modifications of the proteins. The stability of the palmitoyl chains on Gα subunits and the geranylgeranyl chain on $G\gamma_2$ subunits was assessed by thin-layer chromatography on LK5D linear-k silica gel thin-layer chromatography (TLC) plates (Whatman). The plates were developed in chloroform/methanol/2.5 M ammonium hydroxide (9:7:2 v/v/v) under nonreducing and strongly reducing conditions (1 mM dithiothreitol, DTT) to remove the hydrophobic modifications.

Fluorescent Probes. All probes were purchased from Molecular Probes, Inc. Concentrated stocks of probes were made in dimethylformamide (DMF) and stored at −20 °C under nitrogen.

Labeling Gα with Coumarin Succinimidyl Ester (SE) and Alexa488 SE. $G\alpha_q$ and $G\alpha_s$ were labeled with the amine-reactive probe coumarin SE by initially raising the pH of the protein solution to 8.0 and adding a small aliquot of the probe dissolved in DMF at a 5:1 probe:protein ratio. After 45 min of incubation, unreacted probe was removed by extensive dialysis at 4 °C in 150 mM NaCl and 20 mM Hepes buffer at pH 7.2, with 1 mM β-mercaptoethanol and 10 μM GDP for $G\alpha_q$ and $G\alpha_s$. A similar method was used for the labeling of $G\alpha_q$ by Alexa 488 SE.

Double Labeling Gα with Dabcyl SE and Acrylodan. Gα was labeled with amine-reactive probe Dabcyl SE after the pH was raised to 8.0, followed by the addition of the probe at a 5:1 probe:protein ratio. Unreacted Dabcyl was removed by dialysis in 150 mM NaCl and 20 mM Hepes buffer at pH 7.2 after 30 min of incubation on ice. This step also removes the β-mercaptoethanol present in the $G\alpha_q$ storage buffer. Labeling by a second, thiol-reactive probe (acrylodan) was carried out by adding probe at a 5:1 probe:protein ratio in the absence of reducing agent and dialyzing unreacted acrylodan in 150 mM NaCl and 20 mM Hepes buffer after 2 h of incubation on ice.

Labeling Gα with Mant-GDP. Gα was labeled with Mant-GDP by incubating Gα with a 4-fold molar excess of probe in a 30 °C water bath for 1 h after the addition of 50 mM Hepes, 100 mM $(NH_4)_2SO_4$, 150 mM $MgSO_4$, 100 mM ethylenediaminetetraacetic acid (EDTA), and 100 nM Mant-GDP. Excess probe was then removed by dialysis in 150 mM NaCl and 20 mM Hepes buffer at pH 7.2 containing 1 mM mercaptoethanol.

Double Labeling Gα with Mant-GDP and Dabcyl. Gα was labeled with amine-reactive probe Dabcyl SE after the pH was raised to 8.0, followed by the addition of the probe at a 5:1 probe:protein ratio. Unreacted probe was removed by dialysis in 150 mM NaCl and 20 mM Hepes buffer at pH 7.2 after 45 min of incubation. We bound Mant-GDP to Gα by incubating it in a 30 °C water bath for 1 h after the addition of 50 mM Hepes, 100 mM $(NH_4)_2SO_4$, 150 mM $MgSO_4$, 100 mM EDTA, and 100 nM Mant-GDP. Excess probe was then dialyzed out in 150 mM NaCl and 20 mM Hepes buffer containing 1 mM β-mercaptoethanol.

Double Labeling G with Fluorescein and CPM. Gα was labeled with the amine-reactive probe fluorescein succinimidyl ester (SE) by raising the pH of the protein solution to 8.0 and adding a small aliquot of probe dissolved in DMF at a 2:1 probe:protein ratio. After 1 h of incubation, the unreacted probe was removed by extensive dialysis in 150 mM NaCl and 20 mM Hepes buffer containing 10 μM GDP at pH 7.2. The second probe, 7-diethylamino-3-(4′-maleimidylphenyl)-4-methylcoumarin (CPM), which labels the cysteines, was directly added to the protein solution at a 2:1

molar ratio. The labeling reaction was quenched after 10 min by the addition of 20 mM β-mercaptoethanol.

Labeling PLCβ_2 with Acrylodan. PLCβ_2 was dialyzed in 20 mM Hepes and 0.15 M NaCl, pH 7.2, followed by the addition of a 4-fold excess of the thiol-reactive probe acrylodan. After incubation at 0 °C for 2 h, the solution is extensively dialyzed against buffer containing DTT to quench the reaction and remove unreacted probe.

Labeling Lipids with Laurdan. LUVs were labeled by the addition of 0.2 mol % Laurdan and sonication at low energy for 2 min.

Gα Activation. Labeled Gα was activated by incubating it in a 30 °C water bath for 1 h after the addition of 50 mM Hepes, 100 mM $(NH_4)_2SO_4$, 150 mM $MgSO_4$, 100 mM EDTA, and 100 μM GTPγS. Activated Gα was then dialyzed into 150 mM NaCl and 20 mM Hepes buffer containing 1 mM β-mercaptoethanol and 10 μM GTPγS (see ref *18*).

Visualization of Gα Binding to Lipid Raft Domains. Monolayers were prepared by mixing 46% POPC, 23% POPS, 30% cholesterol, and 1% Texas Red phosphoethanolamine (TR-PE) in chloroform and carefully adding the mixture to a circular Teflon trough 50 mm in diameter, containing 10 mL of 150 mM NaCl, 20 mM Hepes, and 1 mM β-mercaptoethanol buffer (pH 7.2) as the subphase. The lipid domains formed were viewed under a Zeiss Axioskop microscope by use of a Texas red filter. The surface pressure of the monolayer, measured on a Wilhelmy plate system, was 17 ± 2 dynes/cm^2. Gα_q labeled with Alexa 488 was injected through a side hole into the subphase and viewed with a fluorescein filter. After the addition of the protein, the subphase was stirred with a stir bar before images of the lipid monolayer and the protein were taken.

Fluorescence Experiments. Fluorescence experiments were carried out on an ISS fluorometer (ISS, Urbana, IL) with samples contained in a 3 mm microcuvette. Experiments consisted of 3−15 trials, which were analyzed with SigmaPlot to obtain an average value for the membrane partition coefficient (K_p). A variety of fluorescence-based methods were used to determine the membrane binding affinities as described below.

(*A*) *Coumarin Fluorescence.* Lipid vesicles were titrated into Coumarin-labeled Gα, and the emission from 380 to 480 nm was recorded; a 360 nm excitation wavelength was used. Emission intensity values were calculated from the area under the curves. Corrections for background scatter were made by subtracting out the intensity obtained by titrating lipid vesicles into the buffer. Corrections for dilution were made, and these values were normalized and fit to a hyperbolic function with SigmaPlot to obtain the membrane partition coefficients.

(*B*) *Laurdan Fluorescence*. Laurdan labeled vesicles were titrated into Gα solution and the Laurdan probes were excited at 340 nm. The emission spectra were scanned from 380 to 510 nm. Data were corrected for background scatter. Changes in emission energy, which were obtained in terms of the shift in the center of mass of the spectra, were normalized and fit to a hyperbolic function by use of SigmaPlot.

(*C*) *Acrylodan Fluorescence.* Lipid vesicles were titrated into acrylodan-labeled PLCβ_2, and the emission from 430 to 600 nm was recorded; a 380 nm excitation wavelength was used. Emission intensity values were calculated from the area under the curves. Corrections for background scatter and dilution were made, and normalized data were fit to a hyperbolic function to obtain membrane partition coefficients.

(*D*) *Fluorescence Resonance Energy Transfer from Acrylodan to Dabcyl on Gα_q*. FRET from acrylodan-labeled Cys to Dabcyl on the N-terminus of Gα_q was monitored as lipid bilayers alone or bilayers containing G$\beta\gamma$ were added. The emission of acrylodan was scanned from 430 to 600 nm after it was excited at 380 nm and corrected by subtracting the background spectra of samples of identical composition except that the protein was replaced with buffer. After correction for dilution, the emission intensity was plotted against Gα_q concentration.

(*E*) *FRET between Mant-GDP and Dabcyl on Gα_q*. The changes in energy transfer from Mant-GDP to Dabcyl was monitored as we added lipid bilayers or bilayers containing G$\beta\gamma$ subunits. We scanned the emission of Mant-GDP from 400 to 510 nm after it was excited at 360 nm. Corrections for background scatter were made by subtracting control emission intensities in which the labeled protein was substituted with buffer. After correction for dilution, the emission intensity was plotted against Gα_q concentration.

(*F*) *FRET between CPM and Fluorescein on Gα_q*. The fluorescein spectrum was taken by exciting the probe at 494 nm and scanning the emission peak from 500 to 600 nm. After the addition of CPM to the fluorescein-Gα, the spectrum was taken from 400 to 600 nm after the CPM donor peak was excited at 384 nm. Changes in energy transfer were monitored after correction for background scatter and dilution. The ratios of the emission peaks at 476 (CPM) and 520 (fluorescein) were taken to calculate the change in FRET when the lipid bilayers in the presence and absence of G$\beta\gamma$ were titrated into the cuvette.

Molecular Modeling. A model of Gα_q was created by use of 3D Jigsaw, with Gα_i(GDP) as the template (PDB code 1GP2). GDP was absent from the models created. The distances for the N-terminal residues to the nearby cysteines and to the GDP binding site on Gα_q were calculated by use of WebLab Viewer. The GDP binding sites were assumed on the basis of the conformations available from the Gα_i structure.

Calculation of the Membrane Partition Coefficient K_p. The K_p values reported here correspond to the apparent partition coefficients in which Gα, or the protein of interest, partitions nonspecifically on the membrane surface, as opposed to forming a specific chemical complex with a particular lipid(s). In most of the studies reported here, we have monitored the membrane binding of fluorescently labeled proteins by changes in the fluorescence properties, which will discriminate between populations of the protein in the aqueous phase versus the membrane surface. We normalize these changes in fluorescence, assuming that at saturation all of the protein is membrane-bound, which appears to be the case for several of the proteins tested (*19*). The normalized curves, whose *y* axis refers to the fraction of protein bound as a function of added membrane (*x*-axis), are then fit to an isothermal binding curve to obtain the membrane partition coefficient.

In the case of Gα subunits labeled with a fluorescent probe, we can measure the relative concentrations of Gα in the aqueous phase $[G\alpha]_s$ and membrane-bound $[G\alpha]_m$ regardless of whether it is associated with a protein partner, such as G$\beta\gamma$, on the membrane surface. The increase in the mem-

brane partition coefficient of Gα when G$\beta\gamma$ is present will depend on its isolated membrane partition coefficient as well as its affinity to G$\beta\gamma$ subunits, which can be expressed in terms of a bimolecular dissociation constant:

$$K_p = [G\alpha_m]/[G\alpha_s] \qquad K_d = [G\alpha_m][G\beta\gamma]/[G\alpha_m - G\beta\gamma]$$

$[G\alpha_{mt}] = [G\alpha_m] + [G\alpha_m - G\beta\gamma]$; total Gα on the surface

$$[G\alpha_{mt}] = [G\alpha_m - G\beta\gamma] + K_p[G\alpha_s]$$

$$K_d = [G\alpha_m][G\beta\gamma]/([G\alpha_{mt}] - K_p[G\alpha_s])$$

$$K_d/[G\beta\gamma] = K_p[G\alpha_s]/([G\alpha_{mt}] - K_p[G\alpha_s])$$

$$[G\alpha_{mt}] - K_p[G\alpha_s] = K_p[G\alpha_s][G\beta\gamma]/K_d$$

$$[G\alpha_{mt}]/[G\alpha_s] = K_p([G\beta\gamma]/K_d + 1)$$

$$K_p = K_p^*(1 + [G\beta\gamma]/K_d) \qquad (1)$$

where K_p^* is the partition coefficient in the absence of G$\beta\gamma$.

Thus, the binding of Gα in the presence of G$\beta\gamma$ will be enhanced by the ratio of the G$\beta\gamma$ concentration over K_d, and eq 1 should apply generally to other protein systems. We have measured the K_d between $G\alpha_q$ and a mixture of G$\beta\gamma$ isotypes purified from bovine brain using fluorescence resonance energy transfer (*17*). In these studies we instead used a preparation of purified $G\beta_1\gamma_2$ from a baculovirus Sf9 system. The K_d obtained for these proteins dispersed in solution is much stronger (i.e., $K_d = 15$ nM) than previous estimates (see Discussion). Thus, the presence of 500 nM G$\beta\gamma$ should increase the partition coefficient of $G\alpha_q$ by a factor of 34.

When a second protein partner of Gα such as PLCβ_2 is also present in addition to G$\beta\gamma$

$$K_p = K_p^*(1 + ([G\beta\gamma]/K_{d_{\beta\gamma}}) + ([PLC]/K_{d_{PLC}}) \qquad (2)$$

where $K_{d_{PLC}} = [G\alpha][PLC]/[G\alpha - PLC]$

RESULTS

Role of Lipids Rafts in Driving Membrane Binding. The presence of lipid rafts may alter the membrane partition coefficient of proteins that will preferentially localize inside or outside lipid rafts due to the preference of a hydrocarbon modification or to the preference of the protein for the fluid phase or raft headgroup. Since G protein subunits have saturated (Gα) or unsaturated (G$\beta\gamma$) hydrocarbon modifications (see ref *12*) and bind to membranes through electrostatic interactions (*5*, *6*), their membrane binding may be affected by lipid rafts.

We monitored the membrane binding by labeling $G\alpha_q$ with an environmentally sensitive probe, coumarin, whose fluorescence intensity and emission energy increase upon lipid binding (*7*). Since the fluorescence intensity was also sensitive to protein−protein association (see below), we used the increase in emission energy to determine the membrane partition coefficient (see Materials and Methods) of coumarin-$G\alpha_q$(GDP) protein [C-$G\alpha_q$(GDP)] subunits to large, unilamellar vesicles with uniform surfaces composed of

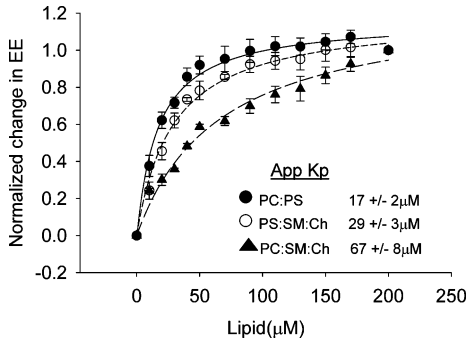

FIGURE 1: Association of 10 nM coumarin-labeled $G\alpha_q$(GDP) with POPC/POPS (2:1) LUVs (●) ($n = 12$), PS/SM/Ch (1:1:1) LUVs (○) ($n = 6$), and PC/SM/Ch (1:1:1) LUVs (▲) ($n = 6$) as determined by the change in emission intensity (*EE*; see Materials and Methods). The normalized emission energies were fit to obtain an apparent K_p as given in the figure. Standard error is shown.

POPC/POPS (2:1) and compared this binding to raft membranes composed of POPS/Ch/SM (1:1:1) at pH 7.2 and 0.15 M NaCl (see refs *20* and *7*). In Figure 1 we show the binding of C-$G\alpha_q$(GDP) to uniform membranes and those that have been shown to form detergent-insoluble fractions (i.e., rafts). A small but significant decrease in binding is seen for the raft membranes. This result contradicts the prediction that the two saturated palmitoyl chains on C-$G\alpha_q$(GDP) would become kinetically trapped in the liquid-ordered raft domains, promoting C-$G\alpha_q$(GDP) binding (*9*). This result correlates well with previous studies that show membrane binding of prenylated G$\beta\gamma$ subunits is unchanged in the presence and absence of rafts (*21*).

The above results show that the presence of rafts does not enhance, and actually slightly inhibits, membrane binding of deactivated Gα subunits. To better understand this result, we viewed the binding of Alexa-labeled $G\alpha_q$(GDP) to monolayers containing 46% POPC, 23% POPS, and 30% cholesterol using fluorescence microscopy (see ref *21*). Monolayers were labeled with Texas Red-PE, which does not partition into raft domains, allowing us to visualize phase separation. Figure 2 shows images of a representative monolayer containing lipid rafts in the presence of 0.1 mol % Alexa-$G\alpha_q$(GDP), viewed by Texas Red fluorescence (Figure 2A) and Alexa fluorescence (Figure 2B). While the Alexa-$G\alpha_q$(GDP) is clearly bound to the monolayer, its binding is uniform, showing no preference between the raft and nonraft domains. Identical results were obtained for $G\alpha_q$(GTPγS) (not shown), implying that activation does not result in preferential binding to rafts. Control studies, shown in Figure 2C,D, were carried out with Alexa 488-Lys_{10}, which has been reported to bind specifically to negatively charged membranes containing $PI(4,5)P_2$ (*22*).

The membrane binding studies of $G\alpha_q$(GDP) shown in Figure 1 indicated a small decrease in binding in the presence of lipid rafts. To understand the reason for this reduction in affinity, we noted that the 33% negatively charged POPS should not be evenly distributed in the presence of 33% cholesterol, and the membrane binding of $G\alpha_q$(GDP) may be reduced under high concentrations of negatively charged lipid. Two studies were done to determine whether this is the case. We first compared the binding of C-$G\alpha_q$(GDP) to uniform and raft membranes where the negatively charged POPS was substituted for electrically neutral POPC lipids.

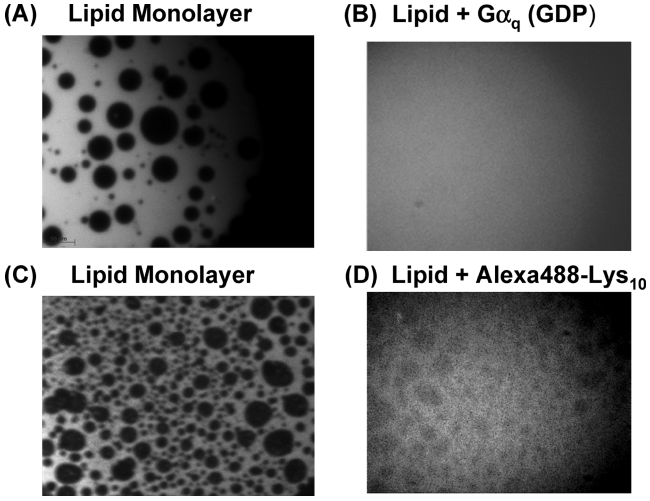

FIGURE 2: (A) Image of a lipid monolayer composed of POPC/POPS/Ch (46:23:30) labeled with 1% Texas red phosphoethanolamine at the air−water interface where the fluid domains are visualized by Texas red PE, which does not incorporate into cholesterol domains. The larger cholesterol are on the order of 50 μm. (B) Image of Alexa-Gα_q(GDP) bound to the surface of the monolayer shown in panel A viewed with a fluorescein filter. (C) Image of a lipid monolayer composed of PS/Ch/PI(4,5)P_2 (69:29:1) containing 1% Texas red phosphoethanolamine, where the fluid domains are visualized by Texas red fluorescence. (D) Image of Alexa488-Lys_{10} binding to PS/Ch/PI(4,5)P_2 (69:29:1) membranes. We note that a higher content of anionic lipid used for the images in panels C and D were required to achieve specific, nonraft binding although some background is still observed, causing the image to be slightly blurred (*22*).

Table 1: Binding of C-Gα_q and C-Gα_s to Model Membranes[a]

species	lipid	K_p (μM)	% charged lipids	*n*
C-Gα_q	PS	30 ± 5	100	4
	PC/PS (2:1)	17 ± 2	33	12
	PS/SM/Ch (1:1:1)	29 ± 3	33	6
	PC	67 ± 8	0	6
	PC/SM/Ch (1:1:1)	67 ± 8	0	6
C-Gα_s	PC/PS (2:1)	73 ± 6	33	6
	PS/SM/Ch (1:1:1)	72 ± 6	33	6

[a] The table compares the membrane partition coefficient of Gα subunits to lipid rafts (e.g., PS/SM/Ch). Also shown is the charge dependence of the G protein subunits to model membranes.

In Table 1, we show that the membrane partition coefficients to both types of neutral membranes are identical although weaker than binding to membranes containing negatively charged lipids. We then measured the binding of C-Gα_q(GDP) to membranes composed entirely of POPS and found it to be weaker than binding to POPC/POPS (2:1). Since monolayer studies show that POPS is sequestered outside raft domains, these results suggest that there is an optimal surface charge that promotes the binding of Gα_q(GDP) to membrane surfaces. The uniform distribution of Gα_q(GDP) on monolayers correlates with the observation that this charge dependence on membrane binding is not very strong, as shown in Table 1.

For comparison, we measured the membrane binding of C-Gα_s(GDP). This G protein subunit was once thought to have one palmitoyl chain, but recent studies have shown a palmitoyl group is linked to the N-terminus (*23*). We compared the binding of C-Gα_s(GDP) to uniform and raft membranes (Table 1). Although the binding constants were much weaker than those values observed for C-Gα_q, we find that the presence of lipid rafts does not affect membrane binding. Taken together, our data show that Gα_q and Gα_s do not bind preferentially to membranes containing lipid rafts.

Table 2: Binding of 10 nM C-Gα_q(GDP) to PC/PS (2:1) Bilayers in the Presence of Protein Partners[a]

partner	K_p (μM)	*n*	K_p (μM) predicted
none	17 ± 2	12	
100 nM G$\beta\gamma$	30 ± 4	18	2.2
500 nM G$\beta\gamma$	25 ± 2	3	0.5
100 nM PLCβ_2	17 ± 5	2	17.0
100 nM G$\beta\gamma$, 100 nM PLCβ_2	44 ± 3	3	2.2
100 nM G$\beta\gamma$, 500 nM PLCβ_2	46 + 4	3	0.5

[a] Comparison of the experimental membrane partition coefficient of Gα_q(GDP) when protein partners are prebound. The predicted values refer to those calculated from the partition coefficient in the absence of a partner, the dissociation constant between the protein and its partner, and the concentration of the protein partner through eq 1.

Contribution of Protein Partners to Membrane Binding of Gα Subunits. To determine the ability of a protein to recruit a partner to the membrane surface, we measured the increase in membrane binding of C-Gα_q(GDP) to PC/PS (2:1) bilayers in the absence and presence of G$\beta\gamma$ subunits. Membrane binding was again assessed by the change in emission energy of the coumarin-labeled protein that occurs upon membrane binding. We note that, in the absence of membranes, association between C-Gα_q(GDP) and G$\beta\gamma$ and PLCβ_2, and between C-Gα_s and G$\beta\gamma$, results in an increase in coumarin intensity without a concomitant change in emission energy.

In Table 2 we list the results of the C-Gα_q(GDP) membrane binding studies. Without G$\beta\gamma$, Gα_q(GDP) binds with a partition coefficient of 17 μM. However, when C-Gα_q(GDP) was premixed with 100 nM G$\beta\gamma$ at a concentration 10-fold higher than the K_d, the partition coefficient showed a small but significant increase to 30 μM, in direct contrast to results predicted by eq 1, which are given in Table 2. The same decrease in the membrane binding affinity was also seen when the concentration of G$\beta\gamma$ was raised to a 50-fold molar excess (Table 2). A weakening in membrane binding is also unexpected because the membrane partition coefficient of the Gα_q(GDP)−G$\beta\gamma$ complex should be the product of the individual partition coefficients of Gα_q(GDP) and G$\beta\gamma$ subunits, but we find that G$\beta\gamma$ subunits also have a strong binding affinity for both POPC and POPC/POPS (2:1) membranes (see Figure 4). We note that for these studies we could only assess binding by monitoring the change in a fluorescent detergent like probe (Laurdan) incorporated into the membrane when G$\beta\gamma$ displaces water upon membrane binding. The observed change in membrane binding with surface charge is in accord with the surface potential studies calculated for transducin G$\beta\gamma$ (*6*).

Instead of premixing the two types of G protein subunits and measuring the binding of the complex, we measured the binding of C-Gα_q(GDP) to PC/PS membranes containing prebound G$\beta\gamma$ subunits at a 1000:1 lipid/protein molar ratio (Figure 3A). The binding experiments were repeated over 15 times. This method gave membrane partition coefficients similar to those obtained when the proteins were premixed and confirm that the presence of G$\beta\gamma$ subunits weakens the membrane binding of Gα_q(GDP) subunits.

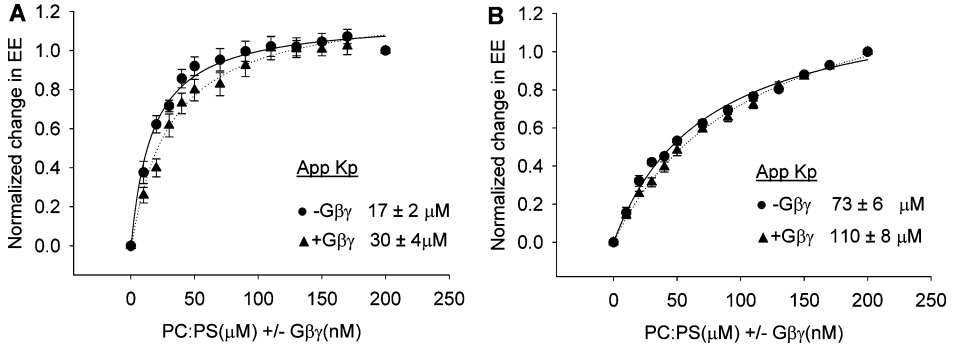

FIGURE 3: (A) Binding of 10 nM coumarin-labeled $G\alpha_q$(GDP) to POPC/POPS (2:1) LUVs (●) and POPC/POPS (2:1) LUVs premixed with $G\beta\gamma$ (▲) ($n = 18$). The data were analyzed by normalizing the change in coumarin emission energy (*EE*; see Materials and Methods) and fitting to a binding curve. (B) Study identical to that in panel A but with $G\alpha_s$(GDP). Standard errors are shown where $n = 6$.

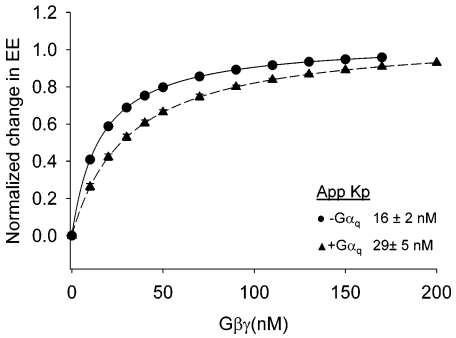

FIGURE 4: Binding of $G\beta\gamma$ to 100 μM Laurdan-labeled POPC/POPS (2:1) LUVs (●) and 100 μM Laurdan-POPC/POPS (2:1) LUVs containing 10 nM $G\alpha_q$(GDP) (▲). The data were analyzed from the shift in center of mass of the Laurdan spectra as $G\beta\gamma$ was titrated into the lipid ($n = 3$), and standard error is shown.

To determine whether the destabilization of membrane binding of C-$G\alpha_q$ by $G\beta\gamma$ occurs with other partners, we repeated the above study using $G\alpha_s$(GDP) (Figure 3B). Taking into account that $G\alpha_s$(GDP) binds to membranes with a lower affinity than $G\alpha_q$(GDP), its membrane binding affinity is similarly reduced by $G\beta\gamma$, suggesting that a similar destabilization mechanism occurs for both types of $G\alpha$ subunits in their deactivated state.

We have carried out a series of studies to understand the reason $G\alpha$(GDP) has a weaker affinity for membranes containing $G\beta\gamma$. We noted that, in general, a large portion of the membrane binding energy of both $G\alpha$ and $G\beta\gamma$ subunits is electrostatic due to positive lobes on their membrane binding faces (*5*, *6*). We thus tested the possibility that the destabilization of $G\alpha$(GDP) by $G\beta\gamma$ is due to charge shielding even though the concentration of negatively charged lipid far exceeds the total amount of the proteins. We tested this idea by measuring the binding of $G\alpha_q$(GDP) to membranes composed entirely of POPS lipids in the absence and presence of $G\beta\gamma$ subunits. Again, a similar behavior was observed (data not shown).

We then measured the binding of $G\beta\gamma$ subunits to POPC/POPS bilayers in the absence and presence of $G\alpha_q$(GDP). We find that the membrane binding of $G\beta\gamma$ is similarly weakened by the presence of $G\alpha_q$(GDP) (Figure 4).

To determine whether the membrane binding affinity of $G\alpha_q$(GDP) decreases in the presence of other protein partners besides $G\beta\gamma$, we measured the change in its affinity in the presence of PLCβ_2. These studies were conducted at a high enough PLCβ_2 concentration that it should be completely complexed with $G\alpha_q$(GDP) (see ref *14*). The data in Table 2 show that, unlike $G\beta\gamma$, the presence of PLCβ_2 does not weaken the membrane binding of $G\alpha_q$(GDP) in accord with predicted results. The fact that PLCβ_2 does not have a strong affinity for unactivated $G\alpha_q$ might contribute to this outcome.

Given that the membrane binding of $G\alpha_q$(GDP)−$G\beta\gamma$ is weaker than its individual components, we attempted to determine whether the association of the $G\alpha_q$(GDP)−$G\beta\gamma$ complex would be strengthened by a second protein partner in accord with thermodynamic predictions (see Table 2). We monitored the binding of C-$G\alpha_q$(GDP)−$G\beta\gamma$ (10 and 100 nM) to membranes containing 0, 100, and 500 nM PLCβ_2. PLCβ_2 has a strong affinity for $G\beta\gamma$ subunits and a weaker affinity for deactivated GDP-$G\alpha_q$ (*14*). As shown in Table 2, our experimental results do not agree with predictions. Rather, the presence of PLCβ_2 in addition to $G\beta\gamma$ resulted in a further reduction in the membrane binding affinity of $G\alpha_q$(GDP).

Membrane Binding Partners of $G\alpha_q$(GDP) May Induce Conformational Changes. The simplest model to explain the unexpected result that $G\beta\gamma$ weakens membrane association of $G\alpha$(GDP) subunits is that $G\alpha$(GDP) exists in two conformational states with different binding affinities. The presence of $G\beta\gamma$ shifts the conformational distribution toward the weaker binding species. Studies on single-Cys $G\alpha_{i1}$ subunits show the N-terminus to be conformationally flexible in the GDP-bound state (*24*). It is thus possible that the lower binding affinity conformation of deactivated $G\alpha_q$ and $G\alpha_s$ is linked to N-terminal flexibility. We also note that $G\alpha_q$ has nine basic residues in its first 32 residues and most models predict this region to be at the membrane interface (*5*). While the crystal structure of activated $G\alpha_i$(GTPγS) shows the N-terminus to be compact around the protein core, this region could not be resolved in the structures of $G\alpha_t$(GDP) and $G\alpha_i$(GDP). Therefore, conformational changes in this region may result in variations in membrane affinity. We first tested whether membrane binding of activated $G\alpha_q$(GTPγS) would be enhanced by the partner proteins $G\beta\gamma$ or PLCβ_2. In Figure 5 we show the results of this study. In contrast to the behavior seen for deactivated $G\alpha_q$, we find that both $G\beta\gamma$ and PLCβ_2 significantly enhance membrane binding of the activated form.

We then determined whether we could observe conformational changes in the N-terminus upon binding to membranes in the absence and presence of protein partners. These studies were carried out by labeling $G\alpha_q$(GDP) with an amine-reactive nonfluorescent energy transfer acceptor (Dabcyl) under conditions where modifications of the N-

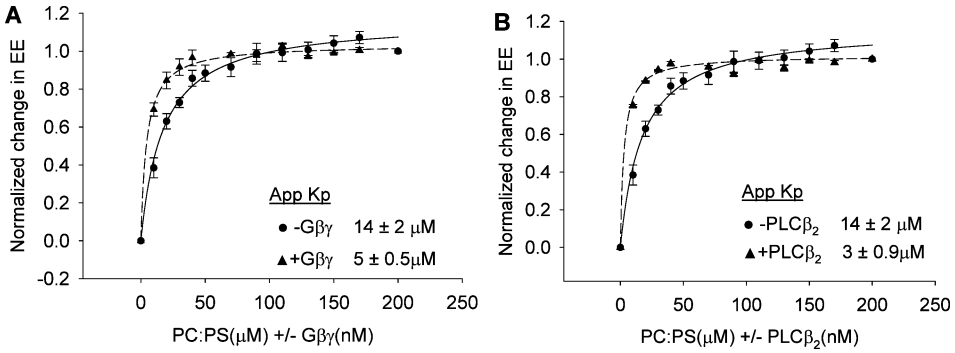

FIGURE 5: (A) Binding of 10 nM coumarin-Gα_q(GTPγS) to POPC/POPS (2:1) LUVs (●) and POPC/POPS (2:1) LUVs with prebound G$\beta\gamma$ (▲). (B) Binding of 10 nM coumarin-Gα_q(GTPγS) to POPC/POPS (2:1) LUVs (●) and POPC/POPS (2:1) LUVs with prebound PLCβ_2 (▲). The data were analyzed from the change in coumarin intensity where $n = 3$, and standard error is shown.

terminus would be favored. The Dabcyl-Gα_q(GDP) was subsequently labeled with a thiol-reactive energy-transfer donor (acrylodan) at a 1:1 probe/protein ratio that would target any one of the three Cys residues in Gα_q or seven Cys residues in Gα_s. We measured the change in fluorescence resonance energy transfer from acrylodan to Dabcyl as the proteins bound to PC/PS (2:1) and PC/PS bilayers containing G$\beta\gamma$ subunits at a 1:1000 lipid/protein ratio. Although it is impossible to construct a molecular picture due to the possibility of heterogeneous labeling of the protein, our results show an increase in acrylodan intensity upon membrane binding, suggesting reduced FRET since the intensity of control samples that were singly labeled with acrylodan did not change (Figure 6A). However, when binding to membranes containing G$\beta\gamma$ subunits, a larger increase in intensity was observed, implying that the presence of G$\beta\gamma$ subunits promotes a different conformational changes in Gα_q(GDP). Similar results were observed for Gα_s(GDP) (data not shown). Repeating this study with the amine-reactive probe fluorescein and the thiol-reactive probe CPM, where $R_0 = 47$ Å (*25*), produced similar results. We then labeled the protein with Dabcyl under conditions that favor modification of the N-terminus and bound the fluorescent energy transfer donor Mant-GDP to Gα_q subunits. However, we do not see energy transfer in this case. Threading models of Gα_q(GDP) based on the structure of Gα_i(GDP) suggest that distance between the N-terminus and the nearest Cys on Gα_q is ~ 50−55 Å (see Figure 6B), whereas that between N-terminus and GDP is 75−80 Å including the contribution of the first ten amino acids, which are missing from the model, suggesting that this large distance is the reason for the lack of FRET between Mant-GDP and the N-terminus.

Presence of Protein Partners Enhances Binding of PLCβ_2. In Figure 5 we show that the presence of G$\beta\gamma$ subunits enhances membrane binding of Gα_q(GTPγS) by the amount predicted by thermodynamics (eq 1). A similar result is also seen for PLCβ_2 (Table 3). To determine whether this is the case for other proteins, we compared the binding of PLCβ_2 to membranes in the presence and absence of G$\beta\gamma$ prebound to the membranes. As seen in Figure 7, its binding was enhanced 2-fold in accord with predictions.

We have previously found that RGS4, which binds strongly to its physiological target Gα_q(GTP), will also bind to PLCβ (*4*). The presence of RGS4 increased the membrane binding of PLCβ_2 3-fold (Table 3), in accord with the idea that RGS4 may bind multiple proteins in the Gα_q signaling system, promoting the formation of membrane-bound complexes of signaling proteins (*4*).

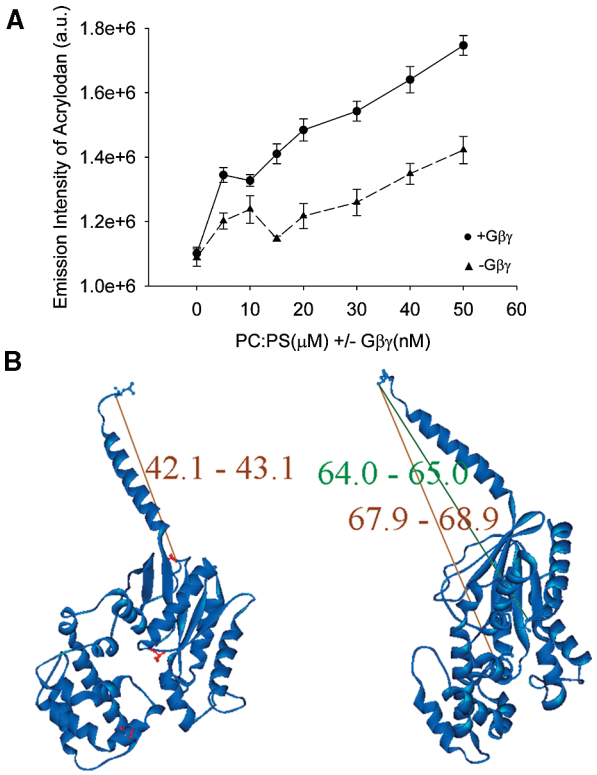

FIGURE 6: (A, top) Extent of FRET between Dabcyl on the N-terminus of Gα_q and acrylodan on the body of Gα_q. The data were analyzed from the acrylodan intensity values as POPC/POPS (2:1) LUVs were titrated without (▲) or with (●) bound G$\beta\gamma$ where $n = 6$ with standard error. (B, bottom) Model of Gα_q represented as a ribbon diagram, with the distance from the amino-terminal atom present to the nearest cysteine and to the GDP binding site shown with WebLab ViewerPro (the first ten amino acids, which are estimated to be 12−16 Å long, are missing from the model).

Changes in Membrane Association with Multiple Partners. Previous studies suggested that some signaling proteins could bind other proteins in their pathway besides their functional partners. We therefore tested whether membrane association can be stabilized by several protein interactions and whether stabilization would be a product of their energies as described by eq 2.

To test this idea, we monitored the membrane binding of several of the proteins in the presence of one and then two partners. The results are listed in Table 3. As can be seen

Table 3: Effect of Multiple Partners in Membrane Partitioning[a]

protein	partner(s)	K_p (μM)
$G\alpha_q$(GTPγS)	none	14 ± 2
	$G\beta\gamma$	5 ± 0.5
	PLCβ_2	3 ± 0.9
	$G\beta\gamma$, PLCβ_2	14 ± 3
PLCβ_2	none	99 ± 6
	$G\beta\gamma$	51 ± 2
	RGS4	28 ± 2
	$G\beta\gamma$, RGS4	62 ± 8

[a] Changes in the membrane partition coefficient of $G\alpha_q$ and PLCβ_2 in the presence of one or two protein partners.

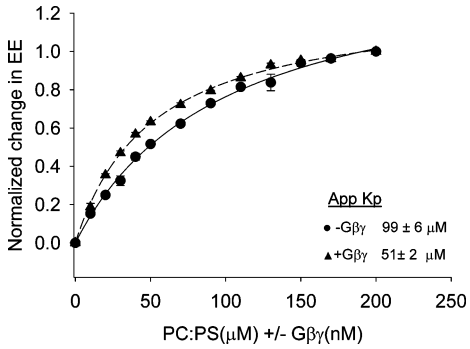

FIGURE 7: Association of 10 nM acrylodan-labeled PLCβ_2 with POPC/POPS (2:1) LUVs (●) and POPC/POPS (2:1) LUVs premixed with $G\beta\gamma$ (▲). Data were analyzed from the area under the spectral curve to give the intensity values for acrylodan, where $n = 6$. Standard error is shown.

for $G\alpha_q$(GTPγS), while the presence of a single partner enhanced membrane binding, the presence of the second decreased the membrane binding when compared to that in the presence of a single partner. An identical result was obtained for the binding of $G\beta\gamma$; membrane binding increased in the presence of prebound $G\alpha$ subunits, but no further increase was seen when PLCβ_2 was also prebound at concentrations far above the dissociation constant. A similar result was obtained for PLCβ_2; the presence of a second partner reduced the membrane binding affinity from that obtained in the presence of one partner only. These data suggest that the binding constant is determined by the enhancement of binding affinity caused by the highest affinity partner. The lack of effect of the lower-affinity partner may result from occlusion of the interaction site. Occlusion of lower-affinity sites has been previously suggested (see refs *26* and *27*).

DISCUSSION

In this study, we have determined the ability of membrane domains and protein partners to drive the membrane binding proteins in the heterotrimeric G protein signaling pathway. Our goal was to link the extensive binding studies of proteins to model membranes to more natural systems and to generate data that may be useful in theoretical models of signal transduction. Here, we focused mainly on G protein subunits since their structure, membrane binding, and protein partners have been fairly well characterized.

We first focused on the potential role of lipid rafts in membrane binding. Since saturated hydrocarbon chains are stabilized in liquid ordered domains through extensive dispersion interactions, we reasoned that $G\alpha_q$(GDP) subunits containing two saturated hydrocarbon chains may preferentially partition into lipid raft domains, and this preferential partitioning would be reflected in the membrane partition coefficient. Instead, monolayer studies show that $G\alpha_q$(GDP) subunits bind to both raft and nonraft domains without apparent preference. We also find that membrane binding of $G\beta\gamma$, $G\alpha_q$(GDP), and $G\alpha_s$(GDP) are not enhanced by rafts (*21*). In fact, the presence of rafts results in a slight loss of membrane binding affinity for $G\alpha_q$(GDP), which may be due to the high local concentration of negatively charged POPS lipids in nonraft domains.

The lack of preference for raft domains in these model membrane systems seems to contradict biochemical studies showing that proteins with two palmitoyl chains such as $G\alpha$ subunits prefer raft domains, whereas $G\beta\gamma$ prefer nonraft domains (*28*, *29*). However, a basic tenet of signal transduction is that, in the basal state, $G\alpha$ subunits are strongly complexed with $G\beta\gamma$ subunits, which would not be the case if the raft partitioning of the two types of subunits differed, unless they form complexes at the raft interface. Our results support the idea that factors besides hydrocarbon modifications are responsible for the apparent preferential partitioning of these subunits.

The absence of partitioning into rafts implies that the hydrocarbon modifications of the G protein subunits may not insert into the lipid matrix in our experiments. The trivial explanation for our results would be that the G protein constructs we have used are not modified. However, previous work comparing prenylated and unprenylated $G\beta\gamma$ subunits show that the lack of modification greatly reduces its PLCβ_2 affinity and its ability to activate this effector (*21*). Our Sf9 $G\beta\gamma$ preparation activates PLCβ_2 well and shows strong PLCβ_2 binding. While the role of hydrocarbon modifications of $G\alpha$ subunits has not been explicitly tested, it is notable that unmodified $G\alpha_s$ expressed in bacteria does not stimulate adenylyl cyclase, whereas Sf9 preparations stimulated adenylyl cyclase but not to the extent of $G\alpha_s$ preparations from tissue extraction (*30*). It is notable that the unusual N-terminal modification of $G\alpha_s$ was only recently discovered (*23*) and it is not clear whether this modification is supported in Sf9 cells. We used identical expression and purification methods for $G\alpha_q$ which have been shown to preserve the palmitoyl modifications. Also, our $G\alpha_q$ preparation is capable of activating PLCβ, which would not be the case if the palmitoyl chains were missing. Transferring this protein into a strongly reducing environment, which reverses palmitoyl linkages, shifted its mobility on a thin-layer chromatography plate.

The energies associated with the insertion of hydrocarbon chains into lipid membranes have been experimentally and theoretically predicted (*32*), and insertion of the hydrophobic modification appears to occur for transducing G proteins (*1*). However, our results seem to suggest that the lipid modifications either do not insert into the lipid matrix or insert equally well into both raft and nonraft domains. Similar partitioning of the palmitoyl chains of $G\alpha_q$ subunits into the two domains may be reasonable considering that the fluid-phase domains contain lipids with one palmitoyl chain. However, the geranylgeranyl group attached to $G\beta\gamma$ subunits would disrupt rafts and so their insertion is unlikely. The crystal structure of prenylated $G\beta\gamma$ shows the prenyl group to be tucked into a small cavity in the protein matrix (*31*), and this same

inclusion in the protein matrix may occur in solution, explaining the lack of effect of rafts on membrane partitioning (*33*), and it has recently been suggested that $G\alpha_t$ subunits contain a prenyl binding site (*34*).

While the membrane binding energies of many signal transduction proteins have been quantified, the role of surface-associated membrane protein partners has not. We have measured the role of partner proteins in driving the membrane binding of a particular protein as a first step in assessing the application of model system parameters to those from more natural systems. The recruitment of a protein to the membrane surface by a partner has been postulated for several pathways in cell signaling (e.g., ref *3*). Membrane recruitment by a protein partner can be predicted by simple thermodynamics, and we find here that these predicted values hold for the increase in membrane binding of activated Gα and PLCβ by membrane-bound partners. In contrast, the presence of protein partners attenuating the membrane binding of deactivated Gα subunits were not predicted by theory. There are at least two mechanisms that may underlie this behavior. One possibility is that deactivated Gα subunits can exist in at least two conformations that have different membrane binding affinities. One conformation is stabilized by the presence of G$\beta\gamma$ subunits and has a weaker membrane binding affinity, whereas the other higher affinity form exists in the absence of G$\beta\gamma$ subunits. Insight into the possible conformational differences comes from previous studies that focused on the highly basic N-terminus of $G\alpha_{i1}$ (*24*). These authors showed that this region, which was unresolved in the crystal structure, undergoes conformational changes upon dissociation from G$\beta\gamma$ subunits and activation. The FRET studies presented here support the idea that the conformation of the N-terminus changes upon membrane binding and that this change differs in the presence of G$\beta\gamma$ subunits. While the molecular details of these changes require further investigation, these results, along with previous ones (*24*), support the idea that the presence of G$\beta\gamma$ subunits promotes an alternate conformation.

An alternate but not exclusive explanation for the decrease in $G\alpha_q$(GDP) and $G\alpha_s$(GDP) membrane binding in the presence of G$\beta\gamma$ subunits is that binding to G$\beta\gamma$ in some way occludes some portion of the membrane binding face. The rates for membrane binding and dissociation of PLCβ and G$\beta\gamma$ have been previously measured (*17*). Assuming that the association rate of Gα(GDP) is similar, then during the time of our measurements, the proteins will undergo many dissociation and reassociation events. Since all of our studies were conducted above the dissociation constant for the Gα(GDP)−G$\beta\gamma$ complex, it is likely that we are viewing the binding of the heterotrimer. This idea is supported by the similar changes in membrane binding for $G\alpha_q$(GDP) in the presence and absence of G$\beta\gamma$, versus those for G$\beta\gamma$ in the presence and absence of $G\alpha_q$(GDP). If the membrane-association sites on Gα(GDP) and G$\beta\gamma$ subunits acted independently when they were free or complexed, then we would expect the membrane partition coefficient to be the product of the individual values, which is clearly not the case. Rather, we find that the membrane binding of the complex is much lower than predicted. Further, if the Gα(GDP)−G$\beta\gamma$ bound to membranes with an affinity that is a product of their individual ones, then the resulting constant would be so high that membrane dissociation would be unlikely. Rather, we find that the weaker binding of the complex may keep the membrane binding energies of the G proteins in a range that would allow dissociation if necessary.

We also find that the membrane binding of G$\beta\gamma$ subunits reciprocally decreases in the presence of $G\alpha_q$(GDP). There are no reports on structural rearrangements of G$\beta\gamma$ upon membrane binding. Also, similar G$\beta\gamma$ structures are observed when bound to $G\alpha_i$ (*35*) and the PH domain of GRK2 (*36*). Thus, we do not expect that the reduction in G$\beta\gamma$ is due to conformational changes, as indicated for $G\alpha_q$. Rather, we suggest that the reduction in binding affinity is due to either occlusion of the membrane binding site or reduction of the charge of the positive lobe that results in strong binding (see ref *6*).

We have also tested the suggestion that a protein may be recruited to the membrane surface by partner as well as nonpartner proteins. If a protein was recruited by multiple protein interactions, then we should see a progressive enhancement of binding as second and their interacting partners are introduced. In the limited survey presented here, this does not appear to be the case; while membrane binding is enhanced by one partner, a second, lower-affinity partner does not result in further enhancement. Thus, membrane stabilization by multiple partners does not occur for the proteins tested here. It can again be argued that multiple interactions may cause the membrane binding energies of these proteins to become so strong that dissociation, which may occur with RGS4 and PLCβ_2, would be prohibitively high.

In summary, the results here provide guidelines for importance of lipid rafts and membrane binding partners in directing the membrane binding of surface-associated signaling proteins. Quantification of these parameters of other systems may ultimately allow for the development of general trends in membrane binding that can be used for predictive methods of signal transduction.

ACKNOWLEDGMENT

We are grateful to Dr. Yuanjian Guo for supplying PLCβ_2 and for her help with the thin-layer chromatography, to Dr. Guillaume Drin for his advice on the energy transfer labeling, to Louisa Dowal for RGS4, and to Marjorie BonHomme and Paxton Provitera for their helpful advice. We are especially grateful to Drs. Stuart McLaughlin and Alok Gambhir for their advice and use of their monolayer apparatus and microscope.

REFERENCES

1. Seitz, H. R, Heck, M., Hofmann, K. P., Alt, T., Pellaud, J., and Seelig, A. (1999) Molecular determinants of the reversible membrane anchorage of the G-protein transducin, *Biochemistry 38*, 7950−60.
2. Arshavsky, V., Lamb, T., and Pugh, E. J. (2002) G proteins and phototransduction, *Annu. Rev. Physiol. 64*, 153−87.
3. Pitcher, J. A., Inglese, J., Higgins, J. B., Arriza, J. L., Casey, P. J., Kim, C., Benovic, J. L., Kwatra, M. M., Caron, M. G., and Lefkowitz, R. J. (1992) Role of $\beta\gamma$ subunits in targeting of the β-adrenergic receptor kinase to membrane bound receptors, *Science 257*, 1264−7.
4. Dowal, L., Elliott, J., Popov, S., Wilkie, T., and Scarlata, S. (2001). Determination of the contact energies between a regulator of G protein signaling and G protein subunits and phospholipase C-β1, *Biochemistry 40*, 414−21.

5. Kosloff, M., Elia, N., and Selinger, Z. (2002) Structural homology discloses a bifunctional structural motif at the N-termini of Gα proteins, *Biochemistry 41*, 14518−23.
6. Murray, D., McLaughlin, S., and Honig, B. (2001) The role of electrostatic interactions in the regulation of the membrane association of G protein beta gamma heterodimers, *J. Biol. Chem. 276*, 45153−9.
7. Scarlata, S. (2002) Regulation of the lateral association of phospholipase C-β2 and G protein subunits by lipid rafts, *Biochemistry 41*, 7092−99.
8. Silvius, J., del Giudice, D., and LaFleur, M. (1996) Cholesterol at different bilayer concentrations can promote or antagonize lateral segregation of phospholipids of differing acyl chain 30 length, *Biochemistry 35*, 15198−208.
9. Schoeder, R., London, E., and Brown, D. (1994) Interactions between saturated acyl chains confer detergent resistance on lipid and glycosylphosphatidylinositiol-anchored proteins, *Proc. Natl. Acad. Sci. U.S.A. 91*, 12130−4.
10. Anderson, R. G. (1998) The caveolae membrane system, *Annu. Rev. Biochem. 67*, 199−225.
11. Moffett, S., Brown, D. A., and Linder, M. E. (2000) Lipid-dependent targeting of G proteins into rafts, *J. Biol. Chem. 275*, 2191−8.
12. Wedegaertner, P., Wilson, P., and Bourne, H. (1995) Lipid modifications of trimeric G proteins, *J. Biol. Chem. 270*, 503−6.
13. Runnels, L. W. (1997). *Regulation of Phospholipase C-β Isozymes by Heterotrimeric GTP Binding Proteins*, State University of New York at Stony Brook, Stony Brook, NY.
14. Runnels, L. W., and Scarlata, S. (1999) Determination of the affinities between heterotrimeric G protein subunits and their phospholipase C-β effectors, *Biochemistry 38*, 1488−96.
15. Rebecchi, M. J., and Pentyala, S. N. (2000) Structure, function, and control of phosphoinositide-specific phospholipase C, *Physiol. Rev. 80*, 1291−335.
16. Rhee, S. G. (2001) Regulation of phosphoinositide-specific phospholipase C, *Annu. Rev. Biochem. 70*, 281−312.
17. Runnels, L. W., and Scarlata, S. F. (1998) Regulation of the rate and extent of phospholipase C-β_2 effector activation of the $\beta\gamma$ subunits of heterotrimeric G proteins, *Biochemistry 37*, 15563−74.
18. Chiadac, P., Mavkin, V. S., and Ross, E. M. (1999) Kinetic control of guanine nucleotide binding to soluble Gαq, *Biochem. Pharmacol. 58*, 39−48, 31.
19. Runnels, L. W., Jenco, J., Morris, A., and Scarlata, S. (1996) Membrane binding of phospholipases C-β_1 and C-β_2 is independent of phosphatidylinositol 4,5-bisphosphate and the α and $\beta\gamma$ subunits of G proteins, *Biochemistry 35*, 16824−32.
20. Xu, X., and London, E. (2000) The effect of sterol structure on membrane lipid domains reveals how cholesterol can induce lipid domain formation, *Biochemistry 39*, 843−9.
21. Fogg. V., Azpiazu, I., Linder, M. E., Smrcka, A., Scarlata, S., and Gautam, N. (2001) Role of the gamma subunit prenyl moiety in G protein beta gamma complex interaction with phospholipase Cbeta, *J. Biol. Chem. 276*, 41787−802.
22. Gambhir, A., Hangyás-Mihályné, G., Zaitseva, I., Cafiso, D. S., Wang, J., et al. (2004) Electrostatic sequestration of PIP2 on phospholipid membranes by basic/aromatic regions of proteins, *Biophys. J. 86*, 2188−207.
23. Kleuss, C., and Krause, E. (2003) G alpha(s) is palmitoylated at the N-terminal glycine, *EMBO J. 22*, 825−32.
24. Medkova, M., Preininger, A. M., Yu, N.-J., Hubbell, W. L., and Hamm, H. E. (2002) Conformational change in the amino-terminal helix of the G protein α_{i1} following dissociation from G$\beta\gamma$ subunit and activation, *Biochemistry 41*, 9962−72.
25. van der Meer, W., Coker, G., and Chen, S. S.-Y. (1994) *Resonance Energy Transfer, Theory and Data*, VCH Publishers, Inc., New York.
26. Clapham, D. E., and Neer, E. J. (1997), G Protein $\beta\gamma$ Subunits, *Annu. Rev. Pharmacol. Toxicol. 37*, 167−203.
27. Hamm, H. (1998) The many faces of G protein signaling, *J. Biol. Chem. 273*, 669−72.
28. Oh, P., and Schnitzer, J. E. (2001) Segregation of heterotrimeric G proteins in cell surface microdomains, *Mol. Biol. Cell 12*, 685−98.
29. McCabe, J. B., and Berthiaume, L. G. (2001) N-terminal protein acylation confers localization to cholesterol, sphingolipid-enriched membranes but not to lipid rafts/caveolae, *Mol. Biol. Cell 12*, 3601−17.
30. Kleuss, C., and Gilman, A. (1997) Gs alpha contains an unidentified covalent modification that increases its affinity for adenylyl cyclase, *Proc. Natl. Acad. Sci. U.S.A. 94*, 6116−20.
31. Hepler, J. M., Biddlecome, G. H., Kleuss, C., Camp, L. A., Hofmann, S. L., et al. (1996) Functional importance of the amino terminus of Gqα, *J. Biol. Chem. 271*, 496−504.
32. Peitzch, R., and McLaughlin, S. (1993) Binding of acylated peptides and fatty acids to phospholipid vesicles: Relevance to myristoylated proteins, *Biochemistry 32*, 10436−43.
33. Loew, A., Ho, Y., Blundell, T., and Bax, B. (1998) Phosducin induces a structural change in transducin betagamma, *Structure 6*, 1007−19.
34. Dietrich, A., Scheer, A., Illenberger, D., Klogg, Y., Henis, Y. I., and Gierschik, P. (2003) Studies on G-protein α-$\beta\gamma$ heterotrimer formation reveal a putative S-prenyl-binding site in the α subunit, *Biochem. J. 376*, 449−56.
35. Wall, M. A., Coleman, D. E., Lee, E., Iniguez-Lluhi, J. A., Posner, B. A., Gilman, A. G., and Sprang, S. R. (1995) The structure of the G protein heterotrimer Gi alpha 1 beta 1 gamma 2, *Cell 83*, 1047−58.
36. Lodowski, D. T., Pitcher, J. A., Capel, W. D., Lefkowitz, R. J., and Tesmer, J. J. (2003) Keeping G proteins at bay: a complex between G protein-coupled receptor kinase 2 and G$\beta\gamma$, *Science 300*, 1256−62.

BI049381+